Supporting Information for Photothermocapillary Oscillators

Adam W. Hauser,[1,*] Subramanian Sundaram,[2,*] and Ryan C. Hayward[1,†]

[1] *Department of Polymer Science and Engineering, University of Massachusetts Amherst, Amherst, MA 01003, USA*

[2] *Department of Electrical Engineering and Computer Science, Massachusetts Institute of Technology, Cambridge, MA 02139, USA*

METHODS

Nanocomposite gel synthesis

Mercaptoundecanoic acid coated gold nanoparticles (AuNPs) are synthesized by the Stucky method with slight modifications.[1] Nanocomposite gels are synthesized as follows: 0.4 mg AuNP are dried in a vial before adding a pre-gel solution comprising 11.7 mg acrylamide, 1.5 mg sodium acrylate, and 0.2 mg methylene bisacrylamide in 200 μL deionized water. The solution is degassed and the reaction is initiated by adding 2 μL of an aqueous ammonium persulfate solution (0.1 g/mL) before injecting between two glass slides separated by 125 μm Kapton spacers. The mold is then placed under N_2 and allowed to react for 1 h. The gels are placed in deionized water to release from the mold, then transferred several times to fresh water solutions to wash. The gels are punched manually into the desired size and shape with stainless steel punches (leathercrafttools.com).

Oscillatory motion experiments

Deionized water droplets (100–300 μL) are placed on polystyrene surfaces and situated on a Nikon ECLIPSE Ti inverted microscope stage. White light from a Lumencore Light Engine is reflected from a 99% mirror in the fluorescence filter turret before being focused onto the droplet surface using a 10x objective lens. Videos are recorded from above with a digital camera at 60 fps. The incident intensity is measured by a power meter and reported intensities are an average reading between 500 and 600 nm. Using a thermocouple immersed in the droplet $\sim$ 1 mm away from submerged (stationary) discs subjected to photothermal heating, we verify that there is a negligible temperature increase in the bulk of the droplet over a time-scale of at least $\sim$ 30 s. However, evaporation of water from the drops is inevitable even at room temperature, and hence a fresh drop is prepared immediately prior to the start of each experiment.

Video descriptions

S1: gel size a=1 mm on a 200 μL drop with a light intensity of 10 W/cm^2
S2: gel size a=1 mm on a 200 μL drop with a light intensity of 40 W/cm^2
S3: gel size a=1 mm on a 100 μL drop with a light intensity of 10 W/cm^2
S4: gel size a=1 mm on a 100 μL drop with a light intensity of 40 W/cm^2
S5: star shaped gel on a 300 μL drop with a light intensity of 40 W/cm^2
S6: 3 gels with a=1 mm on a 200 μL drop with a light intensity of 40 W/cm^2

Oscillator model

To understand the nonlinear dynamics of the photothermocapillary oscillator, we construct a deterministic model and numerically simulate the equation of motion coupled with the heat transport equation - for the gel disc bound to the water-air interface. The force required to detach the disc from the fluid interface is many orders higher than any other forces in the system, and thus we assume that the gel disc is constrained to move along the interface alone and solve the full system of equations in the s-coordinate defined in Fig. S1A. The multiple forces acting on the disc are shown in Fig. S1B. In short, the Marangoni force drives the disc away from the beam (and the apex) while the capillary force acts as the restoring force. Instead of reaching a steady-state position at the periphery of the beam (where the capillary force is exactly balanced by a quasi-static Marangoni force), the disc exhibits various regimes of sustained oscillations analogous to a Duffing oscillator due to the force nonlinearities. A linear model for the small oscillation regime can be intuitively understood, and is explained in a later section.

To compute the capillary forces, we start by solving the Laplace equation to generate the axisymmetric sessile drop shape for the specified volume of the droplet[2]. For axisymmetric fluid interfaces, the following system of ordinary differential equations (ODEs) can be solved for the desired droplet volume while terminating the simulation on reaching the three phase contact angle of the system ($\theta_c = 87^\circ$, water-polystyrene interface in air):

$$\frac{dx}{ds} = cos\ \theta,\ \frac{dz}{ds} = sin\ \theta, \tag{1a}$$

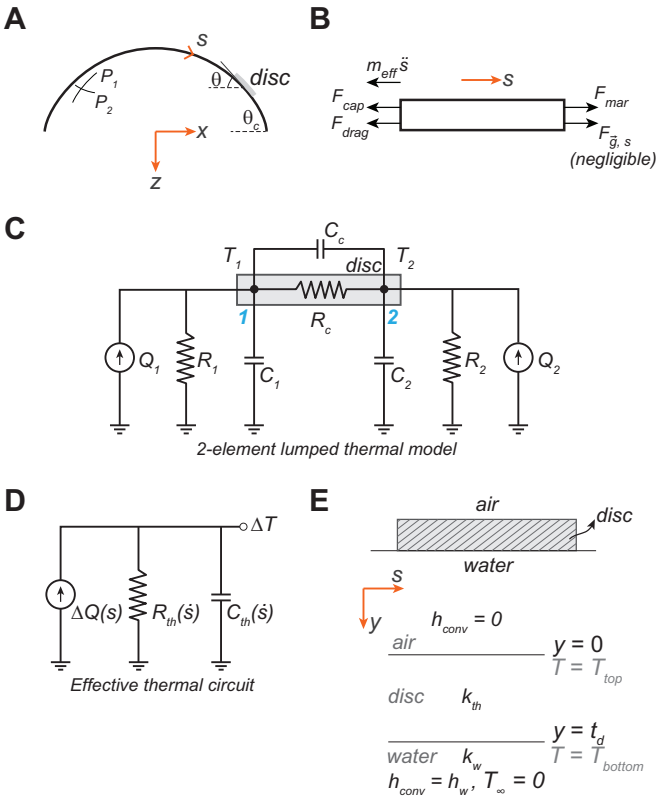

FIG. S1. Photothermocapillary oscillator model A. Model coordinate system B. Forces acting on the gel disc. C. Equivalent 2-element lumped thermal model of the gel disc. R_c is the resistor coupling the two nodes, and is very large when compared to the nodal resistors R_1 and R_2. This is because R_c denotes the resistance for heat transfer by conduction across the diameter of the gel while the nodal resistors represent the resistance to heat flow between the gel disc and water by forced convection. For our disc geometry, the diameter a is much larger than the thickness t_d ($a \gg t_d$). Similarly C_c the coupling capacitor can be ignored to good approximation for our system. This allows simplification of the model to the equivalent differential circuit as shown in D. Here, ΔQ is the differential heat input across the nodes, leading to a temperature difference of ΔT. E. A simplified model used for extracting the effective thermal capacitance at the disc-water interface when heat loss is predominantly set by convection.

$$\frac{d\theta}{ds} = \begin{cases} \beta, & s = 0 \\ 2\beta + \gamma_c z - \frac{sin\ \theta}{x}, & \text{otherwise} \end{cases} \tag{1b}$$

$$\frac{dV}{ds} = \pi x^2 sin\ \theta,\ \frac{dA}{ds} = 2\pi x \tag{1c}$$

where β is the curvature at the origin, γ_c is the capillary constant ($\Delta\rho \cdot g/\gamma$), V is the volume and A is the surface area. The first principal curvature P_1 is equivalent to curvature of the plane curve, given by $\frac{d\theta}{ds}$, and the second principal curvature $P_2 = \frac{sin\ \theta}{x}$. The mean ($H_0$) and deviatoric ($\Delta c_0$) curvatures are given by

$$H_0 = \beta + \frac{\gamma_c z}{2}$$
$$\Delta c_0 = \begin{cases} 0, & s = 0 \\ 2\beta + \gamma_c z - \frac{2sin\ \theta}{x}, & \text{otherwise} \end{cases} \tag{2}$$

The capillary force F_{cap} is obtained from the derivative of the energy of adsorbing a disc to a curved interface [3–5], as

$$F_{cap} = -\frac{\pi\gamma a^4}{8}\frac{d}{ds}\left(\Delta c_0^2 + 2H_0^2\right) \tag{3}$$

where γ is the surface tension and a is the diameter of the disc. For the sessile drop in our setting, with $\theta_c = 87°$, the capillary force is always negative, indicating its restoring nature.

The intensity and the temporal properties of the Marangoni force, $F_{mar} \approx \gamma_T a \Delta T$, are largely set by the thermal behavior of the system. Using lumped system analysis, it is straightforward to calculate the thermal time constant, τ_{th} for objects with a uniform temperature with heat transfer dominated by convection, to be given by

$$\tau_{th} = \frac{m_{eff} c_p}{h_w A_s} \tag{4}$$

where m_{eff} is the effective mass of the object, c_p is the specific heat capacity, h_w is the convection heat transfer coefficient and, A_s is the surface area. However, the main challenge here is that the convection heat transfer coefficient in our system varies significantly with velocity. We therefore solve the thermal transport problem coupled with the equation of motion using a velocity dependent heat transfer coefficient. The average convection heat transfer coefficient h_w can be written as a function of the velocity $\dot{s}$, using a flow over a flat plate approximation [6], as

$$h_w(\dot{s}) = 0.664 Pr^{\frac{1}{3}} k_w \sqrt{\frac{\rho_w |\dot{s}|}{a\mu_v}} \tag{5}$$

where Pr is the Prandtl number ($c_p\mu_v/k_w$), k_w is the conductive heat transfer coefficient of water, μ_v is the dynamic viscosity of water and ρ_w is the density of water.

When a light source (eccentric to the disc) is turned on, the Marangoni force is related to the temperature difference between the leading edge and the trailing edge of the gel disc. We begin by treating the light source to be a perfect Gaussian beam (in the x-coordinate system) centered at the apex of the droplet. The differential light input between the leading edge and trailing edge of the disc on the air-water interface, for a full beam width, b, can be written as

$$\Delta I = \alpha I_0 \left(e^{-\frac{8}{b^2}\left(x - \frac{a}{2}cos\theta\right)^2} - e^{-\frac{8}{b^2}\left(x + \frac{a}{2}cos\theta\right)^2} \right) \tag{6}$$

where α is the absorption constant for the particular gel thickness, and I_0 is the peak intensity of the beam. In our experimental setup, $I_0 = 40$ W/cm^2 and $\alpha \approx 0.2$ [7]. To the first order, the thermal system requires a minimum of two lumped nodes and can be represented using the electrical equivalent circuit diagram in Fig.S1C using the standard analogies between the thermal domain circuit parameters and electrical domain. Given the symmetry of the system, we expect the lumped nodal parameters - effective thermal capacitances C_1 and C_2 and the thermal resistances R_1 and R_2 - to be identical. When $a \gg t_d$ and convection loss to water is the predominant mode of heat transfer, the effective circuit for the temperature difference between the nodes can approximated as in Fig. S1D, where $\Delta Q(s)$ is the position dependent differential heat generation between the leading edge and the trailing edge. The effective thermal resistance R_{th}, and the thermal capacitance C_{th}, of each node are velocity dependent. Under conditions where the minimal thermal resistance is set by the convection through water, the instantaneous thermal resistance for a surface of area A_s can be written as $R_{th}(\dot{s}) = (h_w(\dot{s})A_s)^{-1}$. We solve the 1D-heat conduction problem with uniform heat generation assuming heat convected to air from the gel to be negligibly small to obtain the steady state temperature profile for the setup in Fig. S1E. Using the obtained temperature profile, we calculate the lumped thermal capacitance at the disc-water interface using energy methods, i.e. the energy required to raise the temperature to T_{bottom} ($T_{bottom} < T_{top}$). The temperature profile through the depth of the gel, and the instantaneous thermal capacitance can be obtained as

$$T(y) = \frac{qt_d^2}{2k_{th}}\left(1 - \frac{y^2}{t_d^2}\right) + \frac{qt_d}{h_w(\dot{s})} \tag{7a}$$

$$C_{th}(\dot{s}) = c_p\rho_m A_s t_d\left(1 + \frac{h_w(\dot{s})\, t_d}{3k_{th}}\right) \tag{7b}$$

where q is the uniform heat generation density, and m is the mass of the gel.

To model the complete dynamics we solve the following coupled system of equations, where $u_1 = s$, $u_2 = \dot{s}$ and $u_3 = \Delta T$ are the state variables:

$$\begin{aligned}
\dot{u_1} &= u_2 \\
\dot{u_2} &= \frac{1}{m_{eff}}\left(\gamma_T a.u_3 + F_{g,s}(u_1) - \eta_{eff}.u_2 - F_{cap}(u_1)\right) \\
\dot{u_3} &= \frac{1}{C_{th}(u_2)}\left(\Delta Q(u_1) - \frac{u_3}{R_{th}(u_2)}\right)
\end{aligned} \tag{8}$$

where η_{eff} is the effective viscous drag coefficient; explicit dependencies of each term are indicated. ΔQ, the differential heat generation between the lumped nodes of the thermal system is obtained by lumping the disc into two identical semicircular halves. The viscous drag coefficient for a disc moving sideways can be estimated by equating it to a sphere with its radius scaled by 0.566 giving $\eta_d = 6\pi\mu_v(0.566a/2)$ [8]. However, it is noteworthy that for both the effective mass, m_{eff} and the drag coefficients in our system there are two factors that play a critical role (i) the effective mass to be moved is expected to be several times the actual mass of the gel disc itself, and, (ii) the size of the gel disc is similar to the droplet size (disc size, $a \sim$ droplet size), and thus re-circulation and the droplet shape (sphericity) play important roles in the drag [9]. We include a scaling factor for the effective mass ($m_{eff} = \Lambda_m m$) and damping coefficient ($\eta_{eff} = \Lambda_d \eta_d$) in our model to appropriately account for these two effects. Specifically, Λ_m accounts for the added mass of water experienced during acceleration of the gel disc while the effective drag multiplier Λ_d is used to represent the viscous drag experienced by the disc in the re-circulation limited, small volume of the droplet. Λ_m and Λ_d are difficult to estimate analytically and are instead used as two fitting parameters (kept constant for a given droplet volume and disc size) - and are listed in Table 2. All other quantities in the model are specified at their estimated values.

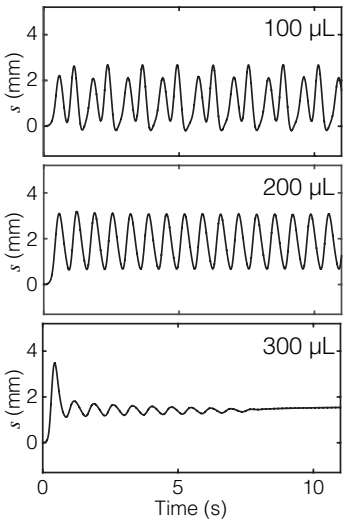

FIG. S2. Model predictions of the disc's center position with time at 10 W/cm^2 incident intensity for the given drop volumes. The simulation settings for these different drop sizes are listed in Table 2. It is important to note that the values of both Λ_d and Λ_m are varied for each drop size. These results show that the behavior seen in experiments can be qualitatively reproduced in simulations, although with two free model parameters that vary with drop size, it is not possible to draw any robust comparisons between experiments and simulations.

Intuitive model and note on the Barkhausen criteria

As the gel disc is differentially heated (differential heat generation, ΔQ) by the beam of light, a temperature difference ΔT is established between the leading and the

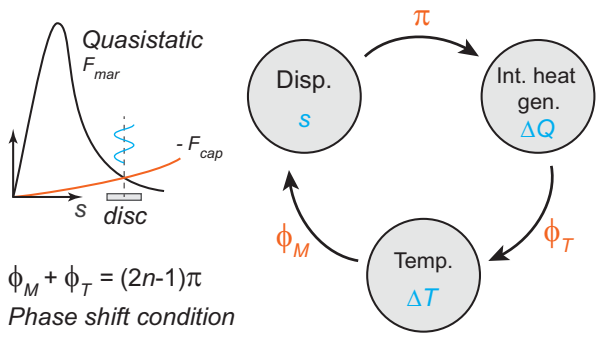

FIG. S3. Schematic illustration of the oscillation cycle. Under small amplitude oscillation conditions, the disc performs oscillations about the point where the quasi-static Marangoni force exactly balances the capillary restoring force. The small signal phase shift between the displacement s and the differential internal heat generation across the two lumped nodes, ΔQ, is exactly π. The thermal and mechanical phase lags are represented by ϕ_T and ϕ_M. The Barkhausen phase shift criterion is then $\phi_M + \phi_T = (2n-1)\pi$.

trailing edge. The resulting Marangoni force causes the disc to move away from the apex ($s = 0$), which reduces the differential heat generation. The capillary force F_{cap} subsequently tries to restore the disc to the apex. Fig. S3 schematically illustrates the feedback mechanism in the oscillation cycle. We define the bias point as the location along the surface of the droplet where the quasi-static Marangoni force exactly balances the capillary force. In the small-amplitude, linear regime of oscillations, the gel disc can be approximated as a harmonic oscillator about this bias point (see Fig. S3). For simplicity, we can consider the heat transport problem to be uncoupled from the equation of motion. Under these settings the Barkhausen criteria can be used to understand the simplified oscillator [10–12]. This implies that the (i) the open-loop gain of the signal is unity in the steady state of oscillations, and (ii) the small-signal phase shift through the system is an integral multiple of 2π [10]. In typical mechanical oscillators, the open-loop unity gain condition is set by amplitude limiting nonlinearities in the system ([11, 13]). The phase shift criterion offers interesting details on the steady state oscillation frequency. This is particularly useful in oscillators where the signal is transduced across multiple domains [11, 12, 14].

In Fig. S3, an infinitesimal movement of the gel disc away from the light source, at the quasi-static equilibrium point, reduces the differential heat generation (ΔQ) in the disc. Therefore, the small-signal phase-shift between the displacement, s, and ΔQ is exactly π. The phase delay of the thermal and mechanical systems are denoted by ϕ_T and ϕ_M respectively. The dynamics of the temperature oscillations are set by the circuit in Fig. S1D, i.e. the phase lag of the small-signal of ΔT with respect to ΔQ is set by the effective thermal circuit parameters, and denoted by ϕ_T. For the first-order thermal system, the phase-lag between the temperature variation and the heat input fluctuations is $\pi/4$ at the cutoff-frequency. This increases to at most $\pi/2$ depending on the frequency of oscillations, i.e. $0 \leq \phi_T \leq \pi/2$. The Marangoni force F_{mar} resulting from the temperature gradient is in phase with the differential temperature across the two nodes, ΔT. Thus the phase delay between ΔT and s in the case of uncoupled equations we consider here, is set purely by the second order equation of motion, where the phase delay (ϕ_M) at the natural frequency is $\pi/2$. At the final frequency of oscillations in this simplified system, the Barkhausen phase-shift criterion (phase shift $= 2n\pi$; $n \in 0, 1, 2...$) becomes $\phi_M + \phi_T = (2n-1)\pi$. The maximum phase-lag arising from the first order thermal system ($\phi_T : \Delta Q \rightarrow \Delta T$) is smaller than $\pi/2$. Therefore the mechanical system has to compensate by adjusting its frequency to produce a phase-lag $\phi_M > \pi/2$. It is therefore required that in the steady state of oscillations the system settles in to an oscillation frequency larger than the natural mechanical frequency (such that $\phi_M > \pi/2$). This frequency offset with respect to the natural mechanical frequency increases with the mechanical damping coefficient. A similar result is observed in an analogous multi-domain self-oscillator [12, 14].

* These authors contributed equally to this work
† hayward@umass.edu

[1] N. Zheng, J. Fan, and G. D. Stucky, J. Am. Chem. Soc. **128**, 6550 (2006).
[2] O. Del Rıo and A. Neumann, J. Colloid Interface Sci. **196**, 136 (1997).
[3] M. Cavallaro, L. Botto, E. P. Lewandowski, M. Wang, and K. J. Stebe, Proc. Natl. Acad. Sci. **108**, 20923 (2011).
[4] P. Galatola, Soft Matter **12**, 328 (2016).
[5] A. Würger, Phys. Rev. E Stat. Nonlin. Soft Matter Phys. **74**, 041402 (2006).
[6] Y. Cøengel, *Heat Transfer: A Practical Approach* (McGraw-Hill, New York, 2002).
[7] A. W. Hauser, A. A. Evans, J.-H. Na, and R. C. Hayward, Angew. Chem. Int. Ed. **54**, 5434 (2015).
[8] H. Lamb, *Hydrodynamics* (Cambridge University Press, Cambridge, 1916).
[9] K. D. Danov, R. Dimova, and B. Pouligny, Phys. Fluids **12**, 2711 (2000).
[10] A. Hajimiri and T. H. Lee, *The Design of Low Noise Oscillators* (Springer Science & Business Media, 1999).
[11] C. Chen, S. Lee, V. V. Deshpande, G.-H. Lee, M. Lekas, K. Shepard, and J. Hone, Nat. Nanotechnol. **8**, 923 (2013).
[12] P. Steeneken, K. Le Phan, M. Goossens, G. Koops, G. Brom, C. Van der Avoort, and J. Van Beek, Nat. Phys. **7**, 354 (2011).
[13] X. Feng, C. White, A. Hajimiri, and M. L. Roukes, Nat. Nanotechnol. **3**, 342 (2008).
[14] S. Sundaram and D. Weinstein, IEEE Trans. Ultrason. Ferroelectr. Freq. Control **62**, 1554 (2015).

TABLE I. Model parameters

α	Optical absorption coefficient of disc
β	Curvature at the apex of the droplet [m^{-1}]
γ	Interfacial tension of air-water interface [$\mathrm{N{\cdot}m}^{-1}$]
γ_c	Capillary constant of water [m^{-2}]
γ_T	Temperature coefficient of surface tension [0.14 $\mathrm{mN{\cdot}m}^{-1}{\cdot}\mathrm{T}^{-1}$]
Δc_0	Deviatoric curvature [m^{-1}]
ΔT	Temperature difference responsible for the Marangoni force [K]
η_{eff}	Effective viscous drag coefficient [$\mathrm{N{\cdot}s{\cdot}m}^{-1}$]
η_d	Viscous drag coefficient of a disk moving sideways [$\mathrm{N{\cdot}s{\cdot}m}^{-1}$]
θ_c	Three phase contact angle (Water-polystyrene-air $\sim 87°$)
Λ_d	Effective drag scaling factor
Λ_m	Effective mass scaling factor
μ_v	Dynamic viscosity [$\mathrm{N{\cdot}s{\cdot}m}^{-2}$]
ρ_m	Density of the gel [$\mathrm{kg{\cdot}m}^{-3}$]
ρ_w	Density of water [$\mathrm{kg{\cdot}m}^{-3}$]
τ_{th}	Thermal time constant [s]
a	Diameter of the gel disc [m]
b	Beam width (Gaussian full beam in simulations) [m]
A_s	Surface area (general) [m^2]
c_p	Specific heat capacity of the gel [$\mathrm{J{\cdot}kg}^{-1}{\cdot}\mathrm{K}^{-1}$]
C_{th}	Effective thermal capacitance [$\mathrm{J{\cdot}K}^{-1}$]
F_{cap}	Capillary force [N]
F_{drag}	Viscous drag force [N]
$F_{g,\dot{s}}$	Effective force due to gravity along s-coordinate [N]
F_{mar}	Marangoni force [N]
H_0	Mean curvature [m^{-1}]
h_w	Convection heat transfer coefficient [$\mathrm{W{\cdot}m}^{-2}{\cdot}\mathrm{K}^{-1}$]
I_0	Peak intensity of gaussian light beam [$\mathrm{W{\cdot}m}^{-2}$]
ΔI	Differential light input across the disc [$\mathrm{W{\cdot}m}^{-2}$]
k_{th}	Conductive heat tranfer coefficient of gel disc [$\mathrm{W{\cdot}m}^{-1}{\cdot}\mathrm{K}^{-1}$]
k_w	Conductive heat transfer coefficient of water [$\mathrm{W{\cdot}m}^{-1}{\cdot}\mathrm{K}^{-1}$]
m_{eff}	Effective mass [kg]
Pr	Prandtl number
P_1	First principal curvature of droplet [m^{-1}]
P_2	Second principal curvature of droplet [m^{-1}]
q	Uniform heat generation density [$\mathrm{W{\cdot}m}^{-3}$]
ΔQ	Differential heat generation across the two nodes [W]
R_{th}	Effective thermal resistance [$\mathrm{K{\cdot}W}^{-1}$]
s	Surface distance [m]
t_d	Thickness of the gel disc [m]

TABLE II. Simulation settings for 1 mm gel disc. Input settings for droplet shape computation, and effective mass and drag scaling coefficients used in the dynamics simulation

Volume	100 µL	200 µL	300 µL
β [m^{-1}]	175.4	109.3	78.4
Λ_d	1.85	2.5	1.72
Λ_m	32.1	23.5	8.9

β is set to obtain the droplet volume with the contact angle fixed (87°) in Laplacian droplet shape computation. Λ_d and Λ_m are varied to account for the role of the added mass and circulation limited flow in small droplet volumes ($a \sim$ droplet size).